Published in final edited form as:
Exp Eye Res. 2013 November ; 116: 63–74. doi:10.1016/j.exer.2013.08.003.

Nanoceria inhibit expression of genes associated with inflammation and angiogenesis in the retina of Vldlr null mice

Svetlana V. Kyosseva[a,*,1], **Lijuan Chen**[a], **Sudipta Seal**[c], and **James J. McGinnis**[a,b,*]

[a]Department of Ophthalmology/Dean McGee Eye Institute, University of Oklahoma Health Sciences Center, Oklahoma City, OK73104

[b]Department of Cell Biology, University of Oklahoma Health Sciences Center, Oklahoma City, OK73104

[c]Advanced Materials Processing Analysis Center, Mechanical Materials Aerospace Engineering, Nanoscience and Technology Center, University of Central Florida, Orlando, FL32816

Abstract

Oxidative stress and inflammation are important pathological mechanisms in many neurodegenerative diseases, including age-related macular degeneration (AMD). The Very Low-Density Lipoprotein Receptor knockout mouse (*Vldlr*−/−) has been identified as a model for AMD and in particular for Retinal Angiomatous Proliferation (RAP). In this study we examined the effect of cerium oxide nanoparticles (nanoceria) that have been shown to have catalytic antioxidant activity, on expression of 88 major cytokines in the retinas of *Vldlr*−/− mice using a PCR array. A single intravitrial injection of nanoceria at P28 caused inhibition of pro-inflammatory cytokines and pro-angiogenic growth factors including *Tslp*, *Lif*, *Il-3*, *Il-7*, *Vegfa*, *Fgf1*, *Fgf2*, *Fgf7*, *Egf*, *Efna 3*, *Lep*, and up-regulation of several cytokines and anti-angiogenic genes in the *Vldlr*−/−retina within one week. We used the Ingenuity Pathway Analysis software to search for biological functions, pathways, and interrelationships between gene networks. Many of the genes whose activities were affected are involved in cell signaling, cellular development, growth and proliferation, and tissue development. Western blot analysis revealed that nanoceria inhibit the activation of ERK 1/2, JNK, p38 MAP kinase, and Akt. These data suggest that nanoceria may represent a novel therapeutic strategy to treat AMD, RAP, and other neurodegenerative diseases.

[*]Corresponding authors: Svetlana V. Kyosseva: Department of Biochemistry & Molecular Biology #516, University of Arkansas for Medical Sciences 4301 West Markham Street, Little Rock, AR 72205, svkiosseva@uams.edu Tel: 1 501 526 4201, Fax: 1 501 603 1146; James F. McGinnis: Department of Ophthalmology/Dean McGee Eye Institute, Department of Cell Biology, University of Oklahoma Health Sciences Center, Oklahoma City, OK 73104, james-mcginnis@ouhsc.edu Tel: 1 405 271 3695, Fax: 1 405 271 3721 .

[1]Present address: Department of Biochemistry & Molecular Biology #516, University of Arkansas for Medical Sciences, 4301 West Markham Street, Little Rock, AR 72205

Keywords

nanoceria; oxidative stress; inflammation; Vldlr mouse; age related macular degeneration; PCR array

1. Introduction

Age-related macular degeneration (AMD) is a leading cause of irreversible blindness in the world (Gehrs et al., 2006). About 1.75 million U.S. residents are affected by AMD and that number is expected to grow to almost 3 million by 2020 (Friedman et al., 2004). AMD is a multifactorial disease that is characterized by degeneration of the retinal photoreceptors, retinal pigment epithelium (RPE), Bruch's membrane, choriocapillaris, and choroidal tissues (Ding et al., 2009). As AMD progresses, it can develop into two distinct forms of late AMD: "dry," atrophic AMD, characterized by RPE senescence and geographic RPE loss, and "wet," neovascular AMD which is characterized by degeneration of RPE and abnormal growth of pathologic choroidal vessels. A defining characteristic of wet AMD, which occurs in about 20% of patients with AMD, is choroidal neovascularization (CNV). A subtype of wet AMD, comprising 10 to 15% of patients with neovascular AMD, is known as retinal angiomatous proliferation (RAP) and is characterized by the presence of subretinal neovascularizations (SRN) and intraretinal neovascularizations (Yannuzzi et al., 2001). Pathogenic mechanisms for AMD include both genetic and environmental factors related to primary RPE senescence, alterations in the complement pathway, changes in the balance of growth factors, excessive lipofuscin accumulation, and oxidative stress (Ding et al., 2009; Zarbin, 2004). There is increasing evidence that oxidative stress, which refers to cellular damage caused by reactive oxygen species (ROS), is involved in the process of photoreceptor cell degeneration (Winkler et al., 1999; Beatty et al., 2000). The retina is highly susceptible to oxidative stress because of its high consumption of oxygen, high metabolic activity and exposure to light. There is also ample evidence that inflammation plays an important role in both "dry" and "wet" AMD (Hollyfield, 2010; Kanda et al., 2008; Telander, 2011). This includes not only mild infiltration of macrophages and accumulation of microglia, but also the presence of inflammatory components such as complement factors, pro-inflammatory cytokines, and chemokines. Many growth factors have been shown to be involved in the development of retinal neovascularization, including vascular endothelial growth factor (VEGF), pigment epithelium-derived factor (PEDF), basic fibroblast growth factor (bFGF, FGF-2), hepatocyte growth factor (HGF), tumor necrosis factor alpha (TNF-α), and others (Kwak et al., 2000; Spilsbury et al., 2000; Lip et al., 2001; Amin et al., 1994; Tomita et al., 2003; Colombo et al., 2007; Qazi et al., 2009; Hu et al., 2009; Dias et al., 2011). A study of genetic linkage and allelic association has identified VEGF, low density lipoprotein receptor-related protein 6 (LRP6) and very low-density lipoprotein receptor (VLDLR) as candidate genes in AMD (Haines et al., 2006).

The VLDLR knockout (*Vldlr−/−)* mouse, with a targeted mutation in the *Vldlr* gene, displayed retinal angiogenesis with new blood vessel formation in the outer plexiform layer extending into the subretinal space (Frykman et al., 1995; Heckenlively et al., 2003). Studies have revealed that spontaneously occurring retinal neovascularization, including intraretinal

neovascularization (IRN), subretinal neovascularization (SRN), and CNV in the *Vldlr*−/− mouse recapitulate many key features in AMD patients who have RAP and can serve as a unique animal model for RAP and other forms of choroidal and retinal neovascularization (Chen et al., 2007; Hu et al., 2008; Jiang et al., 2009; Xia et al., 2011). We (Li et al., 2007; Zhou et al., 2011) and others (Chen et al., 2007; Dorrell et al., 2009) have demonstrated that VEGF expression is elevated in *Vldlr*−/− mouse retinas and VEGF is believed to be involved in the SRN lesions and their leakiness. *Vldlr*−/− retina also shows photoreceptor degeneration, activation of Müller cells around the lesion area, and up-regulation of several pro-inflammatory cytokines (Li et al., 2007; Chen et al., 2009). Furthermore, Chen and colleagues (Chen et al., 2007) have provided evidence that Vldlr knockout resulted in up-regulation of low-density lipoprotein receptor-related protein (LRP 5/6) in the retina and RPE and abnormal activation of the Wnt signaling pathway. It is well known that Wnt signaling is a strong activator of mitochondrial biogenesis and therefore can lead to increased production of ROS known to cause DNA and cellular damage (Zhou et al., 2013).

Cerium is a rare earth element in the lanthanide series of the periodic table. The mechanism underlying the catalytic antioxidant action of cerium oxide nanoparticles (3-5 nm diameter) or nanoceria is generally thought to involve their dual oxidation states (Patil et al., 2006). The loss of oxygen and the reduction of Ce^{4+} to Ce^{3+} are accompanied by creation of oxygen vacancies. The ability of nanoceria to switch between oxidation states is comparable to that of biological antioxidants (Karakoti et al., 2008). This capability imparts nanoceria with the very important biological property of regenerative radical scavenging. The catalytic destruction or scavenging of ROS by cerium oxide nanoparticles (Chen et al., 2006) mimics the activities of antioxidant enzymes superoxide dismutase and catalase (Korsvik et al., 2007; Karakoti et al., 2010) and has potential use in numerous biological applications. Recently nanoceria were shown to have neuroprotective (Das et al., 2007; Estevez et al., 2011), radioprotective (Tarnuzzer et al., 2005; Chen et al., 2006), cardioprotective (Niu et al., 2007) and anti-inflammatory properties (Hirst et al., 2009).

Data from our laboratory have shown that injection of nanoceria into the vitreous, prevents increases in retinal ROS, light damage and blindness in albino rats (Chen et al., 2006) as well as inhibiting the rate of progression of inherited retinal degeneration in the tubby mouse model (Kong et al., 2011). Nanoceria also inhibit: the rise of ROS in the *Vldlr*−/− retina; increases in VEGF in the photoreceptor layer; and the formation of intraretinal and subretinal neovascular lesions (Zhou et al., 2011). In the present study, we analyzed the expression of 88 genes associated with cytokine signaling in the *Vldlr*−/− mouse retina. We demonstrate that nanoceria injected in the newly matured (P28) retina cause a significant and differential modulation in the transcriptional response of multiple cytokine and growth factors genes and inhibit the activation of mitogen-activated protein (MAP) kinases and Akt in the *Vldlr*−/− retina within one week. Consistent with the ability of nanoceria to inhibit neovascular lesions, many of the genes that are up-regulated are either growth factor genes (neuroprotective) or anti-angiogenic or anti-inflammatory genes. Many of those that are down-regulated are pro-angiogenic.

2.1. Animals

Breeding pairs of mutant mice with targeted deletion of the Vldlr gene (B6;129S7-*Vldlr*^{tm1Her}/J; *Vldlr*−/−) were obtained from the Jackson Laboratory (Bar Harbor, ME). These mutants are on a mixed C57Bl/6J X 129S1/SvImJ background. We (Zhou et al., 2011) and others (Chen et al., 2007; Hu et al., 2008; Jiang et al., 2009, Chen et al., 2009) used C57Bl/6J mice as Wt controls. All animals were maintained in a 12 h light-dark cycle with lighting intensity of 80 lx (lux). Animals were cared for and handled according to the Association for Research in Vision and Ophthalmology statement for the use of animals in vision and ophthalmic research and with animal use protocols approved by Oklahoma Health Sciences Center (OUHSC) and Dean McGee Eye Institute Institutional Animal Care and Use Committees (IACUC).

2.2. Intravitreal injection of nanoceria

Mice (*Vldlr*−/− or Wt) at P28 were anesthetized, pupils dilated, a topical anesthetic applied to the cornea and 1 l of 1 mM (172 ng) cerium oxide nanoparticles (nanoceria) in saline was injected into the vitreous under an ophthalmic operating microscope. Cerium oxide nanoparticles were synthesized using simple wet chemistry methods as described previously (Karakoti et al., 2008). Both eyes of each animal received the same treatment. Animals were euthanized at 7 days post injection, and the eyes were rapidly enucleated. Cornea, iris, and lens were removed from the eyecup and then the retina was carefully dissected free of the rest of the eye. The retinas were snap-frozen in liquid nitrogen before storage at −80 °C.

2.3. Real-time PCR

Total RNA was isolated from individual P35 retinas from 4-6 mice of each group (uninjected and injected with nanoceria *Vldlr*−/− or Wt) by STAT-60 reagents according the manufacturer's protocol (TEL-TEST, Inc., Friendswood, TX). Total RNA was eluted in RNase-free water and stored at −80 °C until further analysis. Purity was analyzed spectrophotometrically using a Nanodrop ND-1000 (ratio OD 260/280 > 1.8) and the integrity was visualized in 1.2% agarose gels with ethidium bromide. One microgram of RNA was reverse transcribed into cDNA using the iscript cDNA synthesis kit according to the manufacture's protocol (Bio-Rad Laboratories, Hercules, CA). The mouse cytokine PCR array (Real Time Primers, LLC, Elkins Park, PA) that contained 88 primer sets of cytokine genes and 8 housekeeping gene primers included: Interleukin family: Il2, Il3, Il4, Il5, Il6, Il7, Il9, Il10, IL11, Il12a, Il12b, Il13, Il15, Il19, Il20, Il21, Il23a, Il24, Il28; Growth factors: Fgf1, Fgf2, Fgf3, Fgf4, Fgf5, Fgf6, Fgf7, Fgf8, Fgf9, Fgf10, Fgf11, Fgf12, Fgf13, Fgf14, Fgf15, Fgf16, Fgf17, Fgf18, Fgf20, Fgf21, Fgf22, Fgf23, Egf, Hgf, Pdgfc, Pdgfd, Igf1, Figf, Ngfb, Gas6, Vegfa, Vegfb, Vegfc; Ephrin family: Efna1, Efna2, Efna3, Efna4, Efna5, Efnb1, Efnb2, Efnb3; Neuregulin family*: Nrg1, Nrg3, Nrg4;* Angiopoietin family*: Angpt1, Angpt2, Angpt4;* Others: Lif, Ifne1, Ifnb1, Ifng, Ifnk, Bdnf, Gdnf, Ntf3, Ntf5, Tpo, Prt, Gh, Epo, Lep, Csf1, Csf2, Csf3, Ctf1, Clc, Zfp91, Osm, Tslp; Housekeeping genes *Actb, B2m, Gapd, Gusb, Hprt1, Pgk1, Ppia*, and *Prl13a were used as controls.* A sample volume of 20 μl containing a 1X final concentration of SYBR green, 1 μl cDNA and 2 μl primers at a concentration of 0.1 μM in 10 mM Tris-HCl (pH 7.5), 0.1 mM EDTA was used for all assays. The 96-well plates were run on iCycler IQ (Bio-Rad Laboratories, Hercules, CA)

using the following protocol: 95 °C for 5 min and 50 cycles at 95 °C for 10s and 58 °C for 45 s. The threshold cycle values for all wells were exported to a blank Excel spreadsheet similar to SABiosciences PCR array data analysis template Excel (SABiosciences, Quagen, Valencia, CA). Results were calculated according to ΔΔCt method (Livak and Schmittgen, 2001) used for PCR array analysis. The normalized ΔCt for each gene of interest (GOI) was calculating by deducting the average Ct of the 8 housekeeping genes (HKG) from the Ct for each GOI. The ΔΔCt for each GOI was calculated by deducting the average ΔCt in the control group from the ΔCt of each GOI. To determine the fold change in gene expression, the normalized expression of the GOI in the experimental group was dived by the normalized expression of the same GOI in the control group. The results are expressed as $2^{-\Delta\Delta Ct}$. If the fold change is greater than 1, the results are presented as a fold up-regulation. If the fold change is less than 1, then the negative inverse of the result is presented as a fold down-regulation. The p-value was calculated based on the Student's t-test.

2.4. Western blot analysis

Three retinas of each group (uninjected and injected with nanoceria *Vldlr*−/− or Wt) at P35 were individually sonicated in 100 μl of 10 mM Tris-HCl, pH 7.2 buffer in the presence of a cocktail of phosphatase (PhosStop) and complete protease inhibitors (Roche, Diagnostics Corp., Indianapolis, IN). The sonicate was centrifuged at 12,000 g for 30 min at 4 °C. The resulting supernatant was used in our experiments. The protein concentration was determined by the Pierce BCA protein assay kit according the manufacturer's instructions (Thermo Fisher Scientific, Rockford, IL). Aliquots of each sample (10 μg of protein) were subjected to 10% SDS-PAGE and after electrophoresis, the proteins were electrophoretically transferred to nitrocellulose membranes in a buffer containing 25 mM Tris-HCl, pH 7.4, 190 mM glycine, and 20% (v/v) methanol. The nonspecific binding of proteins was blocked with 5% nonfat dry milk in Tris-buffered saline/0.1% Tween-20 (TBST), pH 7.5 for 1 h at room temperature. The membranes were incubated overnight at 4 °C with polyclonal antibodies diluted 1:1000 in TBST containing 5% BSA. We used the following antibodies from Cell Signaling Tech. (Danvers, MA): phospho-p44/42 MAPK (ERK 1/2) (catalog #9101) that detects endogenous levels of p44 and p42 ERK1/ERK2 when phosphorylated either individually or dually at Thr202 and Tyr 204; p44/42 MAPK (ERK 1/2) (catalog #9102) detects endogenous levels of total p44/42 ERK1/2 protein; phospho SAPK/JNK (catalog #9251) detects endogenous levels of p46/p54 SAPK/JNK1/2 dually phosphorylated at Thr183 and Tyr185; SAPK/JNK (catalog #9252) detects endogenous levels of p46/54 SAPK/JNK1/2 protein; phospho-p38 MAP kinase (catalog #9211) detects endogenous levels of p38 MAPK only when activated by phosporylation at Thr180 and Tyr 182; p38 MAP kinase (catalog #9112) detects endogenous levels of total p38 MAPK protein; phospho-Akt (catalog #9271) detects endogenousl levels of Akt1 only when phosphorylated at Ser473; Akt (catalog #9272) detects levels of total Akt1 protein. After several washings the blotted membranes were incubated with horseradish peroxidase-conjugated anti-rabbit IgG, diluted 1:2000 in TBST containing 5 % milk for 1 h at room temperature. After several washings, bands were detected using the ECL assay and the Kodak 400R image station. When needed, the blots were reprobed with a monoclonal anti-β-actin peroxidase-conjugated antibody (Sigma-Aldrich, St. Louis, MO) diluted 1:10,000 in TBST containing 5% milk. Densitometric analysis of the blots were performed and data were analyzed using GraphPad

Prism, version 5 (San Diego, CA). Two-way ANOVA was used for comparison between groups, followed by a Bonferonni post-test. Statistical significance was set at $p<0.05$.

2.5. Network and functional pathway analysis

Differentially expressed genes were analyzed using Ingenuity Pathway Analysis (IPA) software (Ingenuity Systems, www.imgenuity.com) to search for possible biological processes, pathways, and networks. This web-based application tool enables mapping of gene expression data to relevant pathways based on their functional annotation and known molecular interactions. Each gene symbol was mapped to its corresponding gene object in the Ingenuity Pathways Knowledge Base (IPKB). Networks of these genes were algorithmically generated based on their connectivity and assigned a score. The score is a numerical value used to rank networks according to how relevant they are to the genes in the data set. Two genes are considered to be connected if there is a path in the network between them. In a graphical representation of a network, genes are represented as nodes, and the biological relationship between two nodes is represented as an edge (line). The intensity of the node color indicates the degree of up- or down-regulation. Genes in uncolored nodes were not identified as differentially expressed and were integrated into the computationally generated networks on the basis of IPKB indicating a relevance to this network. The functional analysis of a network identified the biological functions/and or diseases that were most significant to the genes in the network, and the functional analysis of the entire data set identified the biological functions and/or diseases that were most significant to the data set. The network of genes associated with the data set that was associated with the biological functions and/or diseases in the IPKB were considered for analysis. “Right-tailed Fisher’s exact test” was used to calculate a p-value determining the probability that each biological function and/or disease assigned to the network or data set is due to chance alone. Canonical pathways analysis identified molecular pathways from the IPA library (part of IPKB) that were most significant to the date set. Genes from the data set that were associated with a canonical pathway in the IPKB were then considered for further analysis. The significance of the association between the data set and the canonical pathway was measured in 2 ways: 1) A ratio of the number of genes from the data set that map the pathway divided by the total number of molecules that map to the canonical pathway; 2) Fisher’s exact test was used to calculate a p-value determining the probability that the association between the genes in the data set and the canonical pathway is explained by chance alone.

3. Results

3.1. Expression of cytokine genes in the retina of Vldlr−/− mouse

Although some studies have demonstrated that several angiogenic and inflammatory cytokines are increased in the retina of *Vldlr* knockout mice (Li et al., 2007; Chen et al., 2009) the expression pattern of cytokines and their functions in the *Vldlr*−/− mice have not been clearly established. Therefore, we determined the cytokine expression pattern in the *Vldlr*−/− retina using a mouse cytokine PCR array that profiles the expression of 88 key cytokine genes. The complete list of this PCR array is shown in the Material and Methods section. We used a real-time PCR to examine the cytokine gene expression profile of retinas isolated from P35 *Vldlr*−/− on a C57BL/6J background and compare it with that of wild type

(Wt), C57BL/6J mice at P35. We have chosen this age of the *Vldlr*−/− mice because the retinal neovascularization is well underway (Zhou et al., 2011). Real-time PCR analysis revealed that at one week post injection there are no significant differences between the uninjected and saline injected Wt mouse retina (data not shown) and therefore only data from the uninjected Wt controls are used. Results are expressed as fold change and indicate relative expression in untreated Vldlr−/− mice vs Wt mice. Forty-two genes had changes in their expression levels (≥ 1.5 fold) in *Vldlr*−/− retina compared to Wt (Table 1). In keeping with the published data in the literature, we decided that changes above the threshold of 1.5 fold were considered large, although only 12 genes were statistically significant ($p<0.05$) and 5 genes showed a trend towards significance ($p<0.1$). Thirty-seven genes were up-regulated and only 5 were down-regulated. The maximum fold changes were 7.8 and −3.4, respectively. The three up-regulated genes that exhibited the highest changes were *Tslp* (7.8 fold, p=0.0851), *Fgf7* (7 fold, p=0.0356), and *Fgf2* (6.8 fold, p=0.0233). In addition, the following genes were up-regulated as well: *Efna3* (1.9 fold, p=0.0283), *Fgf9* (1.8 fold, p=0.0402), *Egf* (1.7 fold, p=0.1051), *Il17* (1.7 fold, p=0.1061), *Vegfa* (1.6 fold, p=0.1340), and *Lep* (1.6 fold, p=0.1701).

3.2. Expression of cytokine genes in the retina of nanoceria injected Vldlr−/− mouse

To determine if nanoceria treatment alters cytokine gene expression, *Vldlr*−/− mice received a single intravitreal injection in both eyes of 1μl of 1 mM (172 ng) cerium oxide nanoparticles suspended in saline at P28. We previously demonstrated (Zhou et al., 2011) that this concentration of nanoceria prevents the increases in ROS and ROS-mediate damage, and inhibits the rise of VEGF in the *Vldlr*−/− retina. One week after a single injection of nanoceria the expression of 35 cytokine genes (≥ 1.5 fold) in the *Vldlr* knockout mouse are altered compared to age-matched Wt. We found that 9 genes had statistically significant changes ($p<0.05$) and 7 had a trend towards significance ($p<0.1$). Twelve genes were up-regulated and 23 were down-regulated with the maximum fold change between 3.1 and −6.2, respectively (Table 2). The top-three down-regulated genes were *Vegfa* (−6.2 fold, p=0.0009), *IL7* (−4.8 fold, p=0.0410), and *Lif* (−4.4 fold, p=0.0192). Nanoceria also reduced the highest up-regulated genes in the *Vldlr*−/− retina (Table 1), such as *Tslp* (−1.6 fold, p=0.1081), *Fgf7* (−1.8 fold, p=0.1030), and *Fgf2* (−1.6, p=0.0670).

3.3. Functional network analysis

To identify the gene function and associated biological process for the differentially expressed genes in the *Vldlr*−/− retinas, we used the IPA software tool. We found that up- and down-regulated genes in the retina of uninjected and nanoceria injected *Vldlr*−/− mice mapped to 8 specific genetic networks with functional relationships. The top 5 networks are shown in Table 3 and 4. We identified 23 genes that form network 1 in uninjected (Table 3) and nanoceria injected (Table 4) *Vldlr*−/− mice. Most of the genes in this network belong to the *FGF* family. Network 1 is associated with cell to cell signaling and interactions, tissue development, cardiovascular development and function. Accordingly, we found that 21 of the genes are overexpressed in the *Vldlr* −/− retina and 16 of them are fibroblast growth factors. Nanoceria treatment down-regulates most of the genes with no changes in the expression of *Fgf8* and *Fgf12*. Of the 16 focus genes in network 2 in the uninjected *Vldlr*−/− retina, 13 were up-regulated including the Ephrin A family (*Efna1-5)*. After nanoceria

treatment 11 of the genes presented in network 2 were down-regulated. This network is associated with cellular assembly and organization, nervous system development and function, and gastrointestinal disease. The highest up-regulated genes in the *Vldlr*−/− retina, *Tslp*, *Fgf7* and *Fgf2* (Table 1), are part of networks 2, 4 and 5, respectively. The top 3 down-regulated genes in the nanoceria injected retinas *Vegfa*, *Il7* and *Lif* (Table 2) belong to network 4 and 3, respectively.

The molecular relationships between genes in top networks from nanoceria injected *Vldlr*−/− retina are shown in a graphical representation in Figure 1. Among the functions and diseases identified by IPKB, we focused on visual system development and function. Network 1 (Fig. 1A) shows that 8 genes (p=2.44E-3 - 4.3E-2) are critical for development of the eye (*Fgf1*, *Fgf8* and *Fgf17*) and lacrimal gland (*Fgf10*), neovascularization of choroid (*Pdgfc*), pathologic angiogenesis of cornea (*Fgf13* and *Figf*), survival of photoreceptors (*Fgf1*), morphology of the eye (*Fgf10*), proliferation of RPE (*Fgf1*), development of neural retina and RPE (*Fgf9*). Five of the 8 genes of this network were down-regulated and 3 were up-regulated in the nanoceria injected retina. Molecules represented in network 1 are regulated by extracellular regulated protein kinase (ERK) 1/2, a member of the mitogen-activated protein (MAP) kinases that are important mediators of signal transduction and play key roles in the regulation of many cellular processes, such as cell growth and proliferation, differentiation, and apoptosis (Kyosseva, 2004). Network 2 (Fig. 1B) demonstrates that the 2 down-regulated genes (p=3.65E-3 - 2.59E-2), *Efna*1 and *Vegfc*, are important for the development and lymphangiogenesis of cornea, and mitogenesis of retinal cells. The central molecule in this network is the ubiquitous transcription factor, nuclear factor kappa B (NfkB) which is involved in regulating many aspects of cellular activity, in stress, injury and especially in pathways of the immune response (Bonizzi et al., 2004). The 2 down regulated genes (p=3.46E-5 - 4.46E-3) in network 4 (Fig. 1C), *Fgf2* and *Vegfa*, are involved in lymphangiogenesis, angiogenesis and neovascularization, growth of RPE cells, and proliferation of lens cells. The central predicted molecule in the network is the anti-apoptotic serine/threonine kinase, Akt which plays a role in the regulation of a diverse array of biological effects, including cell proliferation, survival, and metabolism (Hers et al., 2011).

3.4. Canonical pathway analysis

Relationships between networks generated by the IPA system and known pathways were investigated by canonical pathway analysis. Canonical pathways that are affected in the functional categories associated with organismal growth and development, and cellular growth, proliferation and development are shown in Figure 2. The most significant pathway in the organismal growth and development category is that for clathrin-mediated endocytosis signaling (Fig. 2A, B). Twenty-four genes are up-regulated in this pathway in the *Vldlr*−/− retina (Fig. 2A) and nanoceria treatment inhibits the expression of 17 genes (Fig. 2B). Accordingly, we found that several signaling pathways, including actin cytoskeleton, ephrin, axonal guidance, macropinocytosis, and HGF signaling are activated in the *Vldlr*−/− retina (Fig. 2A) and nanoceria were able to inhibit them (Fig. 2B). The pathways most relevant to cellular growth, proliferation, and development such as VEGF, mTOR, ILK, and PDGF signaling were activated in the retina of the Vldlr knockout mouse (Fig. 2C) and inhibited by nanoceria treatment (Fig. 2D). It is interesting to note that 19 of the genes in the top

canonical pathway, FGF signaling, were up-regulated and only 2 were down-regulated. After injection with nanoceria, 9 of the genes in this pathway were up-regulated and 12 were down-regulated.

3.5. Nanoceria inhibit MAP kinase activation

Pathway analysis indicated that ERK 1/2 is involved in network 1(Fig. 1A). On the other hand, studies from our laboratory have shown that phosphorylated ERK 1/2 were significantly greater at about 2.5 fold in the retina of 3 week old Vldlr knockout mouse compared to Wt (Li et al., 2007). Therefore, we examined whether MAP kinase signaling pathways are altered in the *Vldlr*−/− and whether nanoceria can affect their activation. The activation of MAP kinases ERK 1/2, c-Jun N-terminal kinase (JNK) 1/2, and p38 were analyzed by Western blot. As shown in Figure 3 (A, D) phosphorylated ERK 1/2 with molecular weight of 44 and 42 kDa, respectively is 4.3-fold greater ($p<0.01$, two-way ANOVA, Bonferonni post-test) and JNK 1/2 with molecular weight of 54 and 46 kDa, respectively (Fig. 3B,E) is 2.6-fold greater ($p<0.001$, two-way ANOVA, Bonferonni post-test) in the retinas of Vldlr knockout mice at P35 compared with those of Wt mice. We observed a modest but significant increase of 1.6-fold ($p<0.001$, two-way ANOVA, Bonferonni post-test) in the phosphorylation of p38 MAP kinase with molecular weight of 38 kDa in *Vldlr*−/− mouse retina when compared to Wt (Fig. 3C, F). A single intravitreal injection of nanoceria for one week reduces the phosphorylation of ERK 1/2 almost to control Wt injected with nanoceria. Nanoceria treatment decreases the phosphorylation of JNK 1/2 to control levels of Wt. Injection of nanoceria dramatically reduced the phosphorylation of p38 almost 10-fold in the *Vldlr*−/− retina and this decrease is below the control levels. The phosphorylation of the three MAP kinases did not show any significant changes after nanoceria treatment in the Wt mice. No detectable changes were determined in the protein levels of ERK 1/2, JNK 1/2 or p38 in all investigated groups (Fig. 3G, H, I). Equal loading was confirmed by reprobing the blots with anti-actin antibody. These results demonstrate that all three members of MAP kinase family are activated differentially in the newly mature retina of the Vldlr knockout mouse and that nanoceria are capable of inhibiting their phosphorylation state.

3.6. Nanoceria inhibit Akt activation

Another kinase predicted by IPA to be a central molecule in network 4 (Fig. 1C) and previously shown to be activated in the *Vldlr*−/− mouse is Akt (Li et al., 2007). We further tested whether Akt is inhibited by nanoceria treatment in the retina. Using a polyclonal antibody that detected predominantly the Akt1 isoform with molecular weight of 60 kDa, we found that phosphorylated Akt was 2.8-fold higher in the *Vldlr*−/− retina at P35 compared to Wt ($p<0.01$, two-way ANOVA, Bonferonni post-test) and nanoceria injection decreased this activation to control levels of Wt mouse with no changes in the levels of non-phosphorylated protein (Fig. 4A, B, C). Similarly these data suggest than Akt is activated in the retina of Vldlr knockout mouse and nanoceria reverse this effect.

4. Discussion

Our study characterizes the expression of several key angiogenic, inflammatory cytokines, and growth factors and defines the protective effect of nanoceria in a mouse model of neovascularization-associated oxidative stress, the *Vldlr*−/− retina. Vldlr is a member of the LDL family and is recognized for its role in neuronal development through reelin signaling. *Vldlr*−/− mice have both choroidal neovascularization coupled with subretinal deposits and photoreceptor atrophy. Due to the global antioxidant properties of cerium oxide nanoparticles, data suggest that nanoceria may reduce cellular structural damage by scavenging and inhibiting ROS, as well as other inflammatory mediators in biological systems (Karakoti et al., 2008; Hirst et al., 2009). In the present study, we have demonstrated a significant and differential modulation of multiple cytokine and growth factor genes after nanoceria treatment in the *Vldlr*−/− retina. The lack of *Vldlr* gene function obviously affects a variety of cell signaling pathways.

4.1. VEGF signaling

VEGFs are the most important regulators of angiogenesis (Ferrara et al., 2003). Previous studies demonstrated elevated mRNA and protein expression of VEGF in *Vldlr*−/− retinas (Dorrell et al., 2009; Hu et al., 2008; Li et al., 2007; Hua et al., 2011) and the overexpression of *Vegf* is found primarily in the ONL surrounding the neovascular lesions (Zhou et al., 2011; Hua et al., 2011). Data from our laboratory have shown that nanoceria prevent the rise in retinal VEGF and the development of vascular lesions in the photoreceptor cell layer of the retina in the *Vldlr*−/− mouse (Zhou et al., 2011). A single injection of nanoceria dramatically reduced the levels of *Vegfa* expression in the Vldlr knockout mouse (Table 2). No significant differences were found in the expression of the other 2 members of VEGF, *Vegfb* and *Vegfc* in uninjected and nanoceria-injected *Vldlr*−/− retinas. Based on IPA data, *Vegfa* is not only involved in VEGF signaling, but in other canonical pathways including clathrin-mediated endocytosis, axonal guidance, Ephrin, Integrin-linked kinase (ILK), mammalian target of rapamycin (mTOR), Il-8, and nitric oxide signaling.

4.2. FGF signaling

FGFs are involved in angiogenesis, wound healing, and embryonic development and play a role in retinal cell proliferation, retinal ganglion cell axon guidance and target recognition, craniofacial patterning, and lens induction (Russell, 2003). FGFs induce a signaling cascade via MAP kinase pathway and protein kinase C (PKC), effectively inducing extracellular matrix (ECM) degradation and angiogenesis via VEGF (Qazi et al., 2009). Our PCR array data demonstrate that most of the genes in FGF family including *Fgf*1, 2, 3, 5, 7, 9, 11, 21, and 22 are overexpressed in the retina of Vldlr knockout mice compared to Wt mice and nanoceria significantly inhibit their expression (Table 3 and 4). The highest up-regulated genes are *Fgf7* and *Fgf 2* (Table 2). Studies have shown that overexpression of FGF7 enhances cell proliferation (Hayashi et al., 2005) and excess of FGF7 in corneal epithelium causes corneal intraepithelial neoplasia in young mice (Chikama et al., 2008). FGF2 is a potent angiogenic molecule in vivo and it is known that VEGF up-regulation can occur in endothelial cells forming capillaries as a consequence of increased FGF-2 expression. While FGF-2 may be one of the initial inducers of endothelial cell proliferation, VEGF, in parallel

or subsequently, is another mediator of this process (Hu et al., 2009). Previous studies demonstrated a strong bFGF staining in the lesion area of the *Vldlr*−/− mouse retina at age 4 weeks. In addition, Western blots showed greater expression of bFGF protein in the knockout mice compared with Wt animals (Li et al., 2007). The most down-regulated gene of the FGF family, after nanoceria injection, was *Fgf9* (Table 2). In the mouse, *Fgf9* is expressed in the distal region of the optic vesicles and plays a role in defining the boundary between neural retina and RPE (Russell, 2003). Another study suggests a role for FGF9 in retinal differentiation and maturation, possibly representing a neuronal derived factor acting upon glial and other cells (Cinaroglu et al., 2005).

4.3. Ephrin receptor signaling and axonal guidance

Ephrin receptors are components of cell signaling pathways involved in axon guidance, cell morphophology and angiogenesis, forming the largest subfamily of receptor tyrosine kinases (Adams and Klein, 2000; Arvanitis and Davy, 2008). An Ephrin signaling network is activated at the optic nerve head after laser-induced ocular hypertension in CD-1 mice (Fu et al., 2010). Microarray analysis of two animal models of retinal angiogenesis, the rat and mouse oxygen-induced retinopathy (OIR), identified increase expression of members of the VEGF, ephrin receptor signaling, and axonal guidance signaling (Recchia et al., 2010). Moreover, soluble Ephrin A2 and Ephrin B4 inhibit retinal neovacularization in an OIR mouse model (Chen et al., 2006; Ehlken et al., 2011). Furthermore, a recent study provides evidence that in Ephrin B2 mutants there is a great reduction of VEGFR phosphorylation and downstream ERK1/2 and Akt activation (Wang et al., 2010). Canonical pathway analysis based on our PCR array demonstrated that 16 genes that make up the Ephrin receptor signaling are up-regulated and only 1 gene is down-regulated in the *Vldlr*−/− retina compared to Wt mice. Nanoceria treatment inhibited all members of the Ephrin signaling in the *Vldlr*−/− retina. Sixteen genes are part of the axonal guidance signaling and 8 of them belong to Ephrin A and Ephrin B family. These results clearly demonstrate the ability of nanoceria to target signaling pathways other than VEGF that have been implicated in both normal retinal vasculogenesis and pathologic neovascularization.

4.4. Endocytosis Pathways

Western blot analysis showed more intense clathrin and adaptin immunoreactivity in AMD donor eyes than were present in non-AMD samples, suggesting that accumulation of clathrin and adaptin in drusen, Bruch's membrane and choroid may reflect a higher rate of clathrin mediated endocytosis in AMD tissues (Bando et al., 2007). In this study we provide evidence that genes in the top canonical pathway in organismal growth and development category, the clathrin-mediated enocytosis pathway, are up-regulated in the uninjected retinas and most of the genes showed decreased expression after nanoceria injections. One of the clathrin-independent endocytic routes is macropinocytosis that is a signal-dependent process normally occurring in response to growth factor stimulation, such as macrophage colony-stimulating factor-1 (CSF-1), epidermal growth factor (EGF), and platelet-derived growth factor (PDGF). Our data present evidence that all these genes are up-regulated in the *Vldlr*−/− retina and down-regulated after nanoceria treatment. Collectively, our findings indirectly suggest that nanoceria may be taken by retinal cells by clathrin-mediated endocytosis and macropinocytosis. Singh and colleagues (Singh et al., 2010) demonstrated

in an *in vivo* uptake study that fluorescein-conjugated nanoceria were taken up by keratinocytes via clathrin, and caveolae-dependent endocytic pathways.

4.5. Cytokines

Several cytokine genes have been demonstrated to be associated with AMD including Il6, Il8, and IL10 (Tsai et al., 2008). Microarray data demonstrated that several genes are up-regulated in Il10 signaling in aged RPE/choroid from mouse (Chen et al., 2008). In our studies, based on IPA canonical pathways, we found that 8 of 9 genes that are part of Il10 signaling pathway are up-regulated in the *Vldlr*−/− retinas and nanoceria injection inhibits the expression of 7 genes. The top up-regulated gene (7.8 fold when normalized against Wt) in the *Vldlr*−/− retina was the Thymic stromal lymphopoietin (*Tslp*) gene. In addition to inhibiting the expression of *Tslp*, nanoceria down-regulates *Il-7* as well. TSLP, is an Il7-like cytokine that plays an important role in initiation and maintenance of the allergic immune response in asthma, inflammatory arthritis, atopic dermatitis, and other allergic states (Liu, 2006; He et al., 2008). A recent study reported that *Tslp* mRNA expression was significantly increased in the cornea epithelia of short ragweed-induced mouse model of allergic conjunctivitis (Zheng et al., 2010). In addition to *Tslp* and *Il7*, another cytokine, *Il9* is elevated to about 1.6 fold in the *Vldlr*−/− retinas and inhibited by nanoceria down to −3.1 fold compared to Wt mice. Il9 plays a role in allergic airway inflammation and autoimmunity (Noelle and Nowak, 2010). Taken together, our results demonstrate that nanoceria are promising therapeutic agents for allergic inflammatory diseases. Another inflammatory cytokine that has high gene expression in *Vldlr*−/− retina is Leukemia inhibitory factor (*Lif*). Injection of nanoceria abolished this overexpression from 5.9 fold in uninjected retinas to −4.4 fold in injected *Vldlr*−/− compared to Wt mice. *Lif* is a member of the Il6 cytokine family and affects cell growth, neural development, embryogenesis, and inflammation. Evidence is provided that, in the retina, *Lif* is up-regulated in response to preconditioning with bright cyclic light leading to increased expression of signal transducer and activator of transcription-3 (STAT3) (Chollangi et al., 2009).

4.6. Kinase signaling pathways

Oxidative stress is well known to induce a number of stress-sensitive signaling proteins including MAP kinases and Akt in human RPE cells (Glotin et al., 2006). We demonstrated in this study that the predicted kinase signaling pathways, such as MAP kinases and Akt, are down-regulated by injection of nanoceria in the *Vldlr*−/− retina. Studies have shown that resveratrol, a plant polyprenol, reduces oxidation and proliferation of human RPE cells and activation of MAP kinase cascades (King et al., 2005) as well as decreasing VEGF-induced phosphorylation of ERK1/2 in vitro and inhibits pathological retinal neovascularization in *Vldlr*−/− mice (Hua et al., 2011).

The cause of AMD is complex and many factors have been implicated including ischemia, oxidative stress, genetics, and inflammation (Telander, 2011). There have been some promising new treatments for AMD in recent years including anti-VEGF; however they have limitations due to the costs of these drugs, their need for frequent injections and possible systemic thromboembolic complications with repeated high dosages of anti-VEGF compounds (Ueta et al., 2009). Several other treatment options are available such as

antioxidant vitamins and mineral supplementations, laser surgery, photodynamic therapy, and low vision aids (Hubschman et al., 2009; Campa et al., 2010). As our understanding of the disease continues to grow at the molecular level, investigators are simultaneously exploring other treatment options that may offer a more long-term solution such as the inhibition of gene expression and signal transduction (Zarbin and Rosenfeld, 2010) or the development of nanoparticle-based drug delivery systems which could be utilized to improve the treatment of neovascular disease in the retina (Farjo and Ma, 2010).

Using inductively-coupled plasma mass spectrometry (ICP-MS), we found that nanoceria were rapidly taken up by rat retina and were preferentially retained in this tissue even after 120 days after a single intravitreal injection (Wong et al., 2013). Our results suggested that the rate of elimination is extremely slow since we observed only 30% reduction of injected nanoceria in the retina after 120 days. We also showed that nanoceria were not toxic to retinal cells over a range of doses used after this long term-exposure.

Our present results show that an array of genes involved in regulating signaling pathways, including VEGF, FGF, Ephrin, MAP kinases, and Akt are up-regulated in *Vldlr*−/− retinas and nanoceria are able to inhibit these changes. Taken together, nanoceria appear to be broad spectrum therapeutic agents for preventing and treating oxidative stress-mediated ocular diseases such as AMD and RAP.

Acknowledgements

This work was supported by grants from: NIH (P30-EY12190, COBRE-P20 RR017703, R21EY018306, R01EY018724); FFB (C-NP-0707-0404-UOK08; NSF: CBET-0708172; OCAST: HR06-075), and unrestricted funds from Presbyterian Health Foundation and Research to Prevent Blindness (RPB). JFM is a recipient of an RPB Senior Scientific Investigator Award.

References

Adams RH, Klein R. Eph receptors and ephrin ligands. essential mediators of vascular development. Trends Cardiovasc. Med. 2000; 10:183–188. [PubMed: 11282292]

Amin R, Puklin JE, Frank RN. Growth factor localization in choroidal neovascular membranes of age-related macular degeneration. Invest. Ophthalmol. Vis.Sci. 1994; 35:3178–3188. [PubMed: 7519180]

Arvanitis D, Davy A. Eph/ephrin signaling: networks. Genes Dev. 2008; 22:416–429. [PubMed: 18281458]

Bando H, Shadrach KG, Rayborn ME, Crabb JW, Hollyfield JG. Clathrin and adaptin accumulation in drusen, Bruch's membrane and choroid in AMD and non-AMD donor eyes. Exp. Eye Res. 2007; 84:135–142. [PubMed: 17097084]

Beatty S, Koh H, Phil M, Henson D, Boulton M. The role of oxidative stress in the pathogenesis of age-related macular degeneration. Surv. Ophthalmol. 2000; 45:115–134. [PubMed: 11033038]

Bonizzi G, Karin M. The two NF-kappaB activation pathways and their role in innate and adaptive immunity. Trends Immunol. 2004; 25:280–288. [PubMed: 15145317]

Campa C, Costagliola C, Incorvaia C, Sheridan C, Semeraro F, De NK, et al. Inflammatory mediators and angiogenic factors in choroidal neovascularization: pathogenetic interactions and therapeutic implications. Mediators Inflamm. 20102010

Chen H, Liu B, Lukas TJ, Neufeld AH. The aged retinal pigment epithelium/choroid: a potential substratum for the pathogenesis of age-related macular degeneration. PLoS ONE. 2008; 3:e2339. [PubMed: 18523633]

Chen J, Hicks D, Brantley-Sieders D, Cheng N, McCollum GW, Qi-Werdich X, et al. Inhibition of retinal neovascularization by soluble EphA2 receptor. Exp. Eye Res. 2006; 82:664–673. [PubMed: 16359662]

Chen J, Patil S, Seal S, McGinnis JF. Rare earth nanoparticles prevent retinal degeneration induced by intracellular peroxides. Nat. Nanotechnol. 2006; 1:142–150. [PubMed: 18654167]

Chen Y, Hu Y, Lu K, Flannery JG, Ma JX. Very low density lipoprotein receptor, a negative regulator of the wnt signaling pathway and choroidal neovascularization. J. Biol. Chem. 2007; 282:34420–34428. [PubMed: 17890782]

Chen Y, Hu Y, Moiseyev G, Zhou KK, Chen D, Ma JX. Photoreceptor degeneration and retinal inflammation induced by very low-density lipoprotein receptor deficiency. Microvasc. Res. 2009; 78:119–127. [PubMed: 19281829]

Chikama T, Liu CY, Meij JT, Hayashi Y, Wang IJ, Yang L, et al. Excess FGF-7 in corneal epithelium causes corneal intraepithelial neoplasia in young mice and epithelium hyperplasia in adult mice. Am. J. Pathol. 2008; 172:638–649. [PubMed: 18276784]

Chollangi S, Wang J, Martin A, Quinn J, Ash JD. Preconditioning-induced protection from oxidative injury is mediated by leukemia inhibitory factor receptor (LIFR) and its ligands in the retina. Neurobiol. Dis. 2009; 34:535–544. [PubMed: 19344761]

Cinaroglu A, Ozmen Y, Ozdemir A, Ozcan F, Ergorul C, Cayirlioglu P, et al. Expression and possible function of fibroblast growth factor 9 (FGF9) and its cognate receptors FGFR2 and FGFR3 in postnatal and adult retina. J. Neurosci. Res. 2005; 79:329–339. [PubMed: 15614790]

Colombo ES, Menicucci G, McGuire PG, Das A. Hepatocyte growth factor/scatter factor promotes retinal angiogenesis through increased urokinase expression. Invest. Ophthalmol. Vis. Sci. 2007; 48:1793–1800. [PubMed: 17389513]

Das M, Patil S, Bhargava N, Kang JF, Riedel LM, et al. Auto-catalytic ceria nanoparticles offer neuroprotection to adult rat spinal cord neurons. Biomaterials. 2007; 28:1918–1925. [PubMed: 17222903]

Dias JR, Rodrigues EB, Maia M, Magalhaes O Jr. Penha FM, Farah ME. Cytokines in neovascular age-related macular degeneration: fundamentals of targeted combination therapy. Br. J. Ophthalmol. 2011; 95:1631–1637. [PubMed: 21546514]

Ding X, Patel M, Chan CC. Molecular pathology of age-related macular degeneration. Prog. Retin. Eye Res. 2009; 28:1–18. [PubMed: 19026761]

Dorrell MI, Aguilar E, Jacobson R, Yanes O, Gariano R, Heckenlively, et al. Antioxidant or neurotrophic factor treatment preserves function in a mouse model of neovascularization-associated oxidative stress. J. Clin. Invest. 2009; 119:611–623. [PubMed: 19188685]

Ehlken C, Martin G, Lange C, Gogaki EG, Fiedler U, Schaffner F, et al. Therapeutic interference with EphrinB2 signalling inhibits oxygen-induced angioproliferative retinopathy. Acta Ophthalmol. 2011; 89:82–90. [PubMed: 19764912]

Estevez AY, Pritchard S, Harper K, Aston JW, Lynch A, Lucky JJ, et al. Neuroprotective mechanisms of cerium oxide nanoparticles in a mouse hippocampal brain slice model of ischemia. Free Radic. Biol. Med. 2011; 15:1155–1163. [PubMed: 21704154]

Farjo KM, Ma JX. The potential of nanomedicine therapies to treat neovascular disease in the retina. J. Angiogenes Res. 2010; 2:21. [PubMed: 20932321]

Ferrara N, Gerber HP, LeCouter J. The biology of VEGF and its receptors. Nat. Med. 2003; 9:669–676. [PubMed: 12778165]

Friedman DS, O'Colmain BJ, Munoz B, Tomany SC, McCarty C, De Jong PT, et al. Prevalence of age-related macular degeneration in the United States. Arch. Ophthalmol. 2004; 122:564–572. [PubMed: 15078675]

Frykman PK, Brown MS, Yamamoto T, Goldstein JL, Herz J. Normal plasma lipoproteins and fertility in gene-targeted mice homozygous for a disruption in the gene encoding very low density lipoprotein receptor. Proc. Natl. Acad. Sci. U.S.A. 1995; 92:8453–8457. [PubMed: 7667310]

Fu CT, Tran T, Sretavan D. Axonal/glial upregulation of EphB/ephrin-B signaling in mouse experimental ocular hypertension. Invest Ophthalmol. Vis. Sci. 2010; 51:991–1001. [PubMed: 19815726]

Gehrs KM, Anderson DH, Johnson LV, Hageman GS. Age-related macular degeneration-emerging pathogenetic and therapeutic concepts. Ann. Med. 2006; 38:450–471. [PubMed: 17101537]

Glotin AL, Calipel A, Brossas JY, Faussat AM, Treton J, Mascarelli F. Sustained versus transient ERK1/2 signaling underlies the anti- and proapoptotic effects of oxidative stress in human RPE cells. Invest. Ophthalmol. Vis.Sci. 2006; 47:4614–4623. [PubMed: 17003459]

Haines JL, Schnetz-Boutaud N, Schmidt S, Scott WK, Agarwal A, Postel EA, et al. Functional candidate genes in age-related macular degeneration: significant association with VEGF, VLDLR, and LRP6. Invest. Ophthalmol .Vis. Sci. 2006; 47:329–335. [PubMed: 16384981]

Hayashi M, Hayashi Y, Liu CY, Tichelaar JW, Kao WW. Over expression of FGF7 enhances cell proliferation but fails to cause pathology in corneal epithelium of Kerapr-rtTA/FGF7 bitransgenic mice. Mol. Vis. 2005; 11:201–207. [PubMed: 15788998]

He R, Oyoshi MK, Garibyan L, Kumar L, Ziegler SF, Geha RS. TSLP acts on infiltrating effector T cells to drive allergic skin inflammation. Proc. Natl. Acad. Sci .U.S.A. 2008; 105:11875–11880. [PubMed: 18711124]

Heckenlively JR, Hawes NL, Friedlander M, Nusinowitz S, Hurd R, Davisson M, et al. Mouse model of subretinal neovascularization with choroidal anastomosis. Retina. 2003; 23:518–522. [PubMed: 12972764]

Hers I, Vincent EE, Tavare JM. Akt signalling in health and disease. Cell Signal. 2011; 10:1515–1527. [PubMed: 21620960]

Hirst SM, Karakoti AS, Tyler RD, Sriranganathan N, Seal S, Reilly CM. Anti-inflammatory properties of cerium oxide nanoparticles. Small. 2009; 5:2848–2856. [PubMed: 19802857]

Hollyfield JG. Age-related macular degeneration: the molecular link between oxidative damage, tissue-specific inflammation and outer retinal disease: the Proctor lecture. Inves.t Ophthalmol. Vis. Sci. 2010; 51:1275–1281.

Hu W, Criswell MH, Fong SL, Temm CJ, Rajashekhar G, Cornell TL, et al. Differences in the temporal expression of regulatory growth factors during choroidal neovascular development. Exp. Eye Res. 2009; 88:79–91. [PubMed: 19013152]

Hu W, Jiang A, Liang J, Meng H, Chang B, Gao H, et al. Expression of VLDLR in the retina and evolution of subretinal neovascularization in the knockout mouse model's retinal angiomatous proliferation. Invest Ophthalmol. Vis. Sci. 2008; 49:407–415. [PubMed: 18172119]

Hua J, Guerin KI, Chen J, Michan S, Stahl A, Krah NM, et al. Resveratrol inhibits pathologic retinal neovascularization in Vldlr(-/-) mice. Invest. Ophthalmol. Vis. Sci. 2011; 52:2809–2816. [PubMed: 21282584]

Hubschman JP, Reddy S, Schwartz SD. Age-related macular degeneration: experimental and emerging treatments. Clin .Ophthalmol. 2009; 3:167–174. [PubMed: 19668561]

Jiang A, Hu W, Meng H, Gao H, Qiao X. Loss of VLDL receptor activates retinal vascular endothelial cells and promotes angiogenesis. Invest. Ophthalmol. Vis. Sci. 2009; 50:844–850. [PubMed: 18936153]

Kanda A, Abecasis G, Swaroop A. Inflammation in the pathogenesis of age-related macular degeneration. Br. J. Ophthalmol. 2008; 92:448–450. [PubMed: 18369057]

Karakoti A, Singh S, Dowding JM, Seal S, Self WT. Redox-active radical scavenging nanomaterials. Chem. Soc. Rev. 2010; 39:4422–4432. [PubMed: 20717560]

Karakoti AS, Monteiro-Riviere NA, Aggarwal R, Davis JP, Narayan RJ, Self WT, et al. Nanoceria as antioxidant: Synthesis and biomedical applications. Jom. 2008; 60:33–37. [PubMed: 20617106]

King RE, Kent KD, Bomser JA. Resveratrol reduces oxidation and proliferation of human retinal pigment epithelial cells via extracellular signal-regulated kinase inhibition. Chem. Biol. Interact. 2005; 151:143–149. [PubMed: 15698585]

Kong L, Cai X, Zhou X, Wong LL, Karakoti AS, Seal S, et al. Nanoceria extend photoreceptor cell lifespan in tubby mice by modulation of apoptosis/survival signaling pathways. Neurobiol. Dis. 2011; 42:514–523. [PubMed: 21396448]

Korsvik C, Patil S, Seal S, Self WT. Superoxide dismutase mimetic properties exhibited by vacancy engineered ceria nanoparticles. Chem. Commun.(Camb.). 2007:1056–1058. [PubMed: 17325804]

Kyosseva SV. Mitogen-activated protein kinase signaling. Int. Rev. Neurobiol. 2004; 59:201–220. [PubMed: 15006489]

Li C, Huang Z, Kingsley R, Zhou X, Li F, Parke DW, et al. Biochemical alterations in the retinas of very low-density lipoprotein receptor knockout mice: an animal model of retinal angiomatous proliferation. Arch. Ophthalmol. 2007; 125:795–803. [PubMed: 17562991]

Lip PL, Blann AD, Hope-Ross M, Gibson JM, Lip GY. Age-related macular degeneration is associated with increased vascular endothelial growth factor, hemorheology and endothelial dysfunction. Ophthalmol. 2001; 108:705–710.

Liu YJ. Thymic stromal lymphopoietin: master switch for allergic inflammation. J. Exp.Med. 2006; 203:269–273. [PubMed: 16432252]

Livak KJ, Schmittgen TD. Analysis of relative gene expression data using real-time quantitative PCR and the 2(-delta delta C(T)) method. Methods. 2001; 25:402–408. [PubMed: 11846609]

Niu J, Azfer A, Rogers LM, Wang X, Kolattukudy PE. Cardioprotective effects of cerium oxide nanoparticles in a transgenic murine model of cardiomyopathy. Cardiovasc. Res. 2007; 73:549–559. [PubMed: 17207782]

Noelle RJ, Nowak EC. Cellular sources and immune functions of interleukin-9. Nat. Rev. Immunol. 2010; 10:683–687. [PubMed: 20847745]

Patil S, Seal S, Guo Y, Schulte A, Norwood J. Role of trivalent La and Nd dopants in lattice distortion and oxygen vacancy generation in cerium oxide nanoparticles. Appl. Phys. Lett. 2006; 88:243110.

Qazi Y, Maddula S, Ambati BK. Mediators of ocular angiogenesis. J. Genet. 2009; 88:495–515. [PubMed: 20090210]

Recchia FM, Xu L, Penn JS, Boone B, Dexheimer PJ. Identification of genes and pathways involved in retinal neovascularization by microarray analysis of two animal models of retinal angiogenesis. Invest. Ophthalmol. Vis. Sci. 2010; 51:1098–1105. [PubMed: 19834031]

Russell C. The roles of Hedgehogs and Fibroblast Growth Factors in eye development and retinal cell rescue. Vis. Res. 2003; 43:899–912. [PubMed: 12668059]

Singh S, Kumar A, Karakoti A, Seal S, Self WT. Unveiling the mechanism of uptake and sub-cellular distribution of cerium oxide nanoparticles. Mol. Biosyst. 2010; 6:1813–1820. [PubMed: 20697616]

Spilsbury K, Garrett KL, Shen WY, Constable IJ, Rakoczy PE. Overexpression of vascular endothelial growth factor (VEGF) in the retinal pigment epithelium leads to the development of choroidal neovascularization. Am. J. Pathol. 2000; 157:135–144. [PubMed: 10880384]

Tarnuzzer RW, Colon J, Patil S, Seal S. Vacancy engineered ceria nanostructures for protection from radiation-induced cellular damage. Nano.Lett. 2005; 5:2573–2577. [PubMed: 16351218]

Telander DG. Inflammation and Age-Related Macular Degeneration (AMD). Semin. Ophthalmol. 2011; 26:192–197. [PubMed: 21609232]

Tomita N, Morishita R, Taniyama Y, Koike H, Aoki M, Shimizu H, et al. Angiogenic property of hepatocyte growth factor is dependent on upregulation of essential transcription factor for angiogenesis, ets-1. Circulation. 2003; 107:1411–1417. [PubMed: 12642363]

Tsai YY, Lin JM, Wan L, Lin HJ, Tsai Y, Lee CC, et al. Interleukin gene polymorphisms in age-related macular degeneration. Invest. Ophthalmol. Vis. Sci. 2008; 49:693–698. [PubMed: 18235016]

Ueta T, Yanagi Y, Tamaki Y, Yamaguchi T. Cerebrovascular accidents in ranibizumab. Ophthalmology. 2009; 116:362. [PubMed: 19187826]

Wang Y, Nakayama M, Pitulescu ME, Schmidt TS, Bochenek ML, Sakakibara A. Ephrin-B2 controls VEGF-induced angiogenesis and lymphangiogenesis. Nature. 2010; 465:483–486. [PubMed: 20445537]

Winkler BS, Boulton ME, Gottsch JD, Sternberg P. Oxidative damage and age-related macular degeneration. Mol. Vis. 1999; 5:32. [PubMed: 10562656]

Wong LL, Hirst SM, Pye QN, Reilly CM, Seal S, McGinnis JF. Catalytic nanoceria are preferentially retained in the rat retina and are not cytotoxic after intravitreal injection. PLosOne. 2013; 8:e58431.

Xia CH, Lu E, Liu H, Du X, Beutler B, Gong X. The role of Vldlr in intraretinal angiogenesis in mice. Invest. Ophthalmol. Vis .Sci. 2011; 52:6572–6579. [PubMed: 21757581]

Yannuzzi LA, Negrao S, Iida T, Carvalho C, Rodriguez-Coleman H, Slakter J, et al. Retinal angiomatous proliferation in age-related macular degeneration. Retina. 2001; 21:416–434. [PubMed: 11642370]

Zarbin MA. Current concepts in the pathogenesis of age-related macular degeneration. Arch. Ophthalmol. 2004; 122:598–614. [PubMed: 15078679]

Zarbin MA, Rosenfeld PJ. Pathway-based therapies for age-related macular degeneration: an integrated survey of emerging treatment alternatives. Retin. 2010; 30:1350–1367.

Zheng X, Ma P, de Paiva CS, Cunningham MA, Hwang CS, Pflugfelder SC, et al. TSLP and downstream molecules in experimental mouse allergic conjunctivitis. Invest. Ophthalmol. Vis. Sci. 2010; 51:3076–3082. [PubMed: 20107175]

Zhou X, Wong LL, Karakoti AS, Seal S, McGinnis JF. Nanoceria inhibit the development and promote the regression of pathologic retinal neovascularization in the vldlr knockout mouse. PLos ONE. 2011; 6:e16733. [PubMed: 21364932]

Zhou Y, Yan H, Guo M, Zhu J, Xiao Q, Zhang L. Reactive oxygen species in vascular formation and development. Oxid. Med. Cell Longev. 20132013:374963. [PubMed: 23401740]

Research Highlights

- Cerium oxide nanoparticles (nanoceria) possess radical scavenging activities.
- Nanoceria inhibit cytokines and angiogenic genes in the retina of Vldlr mouse
- Nanoceria inhibit the activation of MAP kinases and Akt.
- Nanoceria may be therapeutically beneficial in human eye diseases.

A

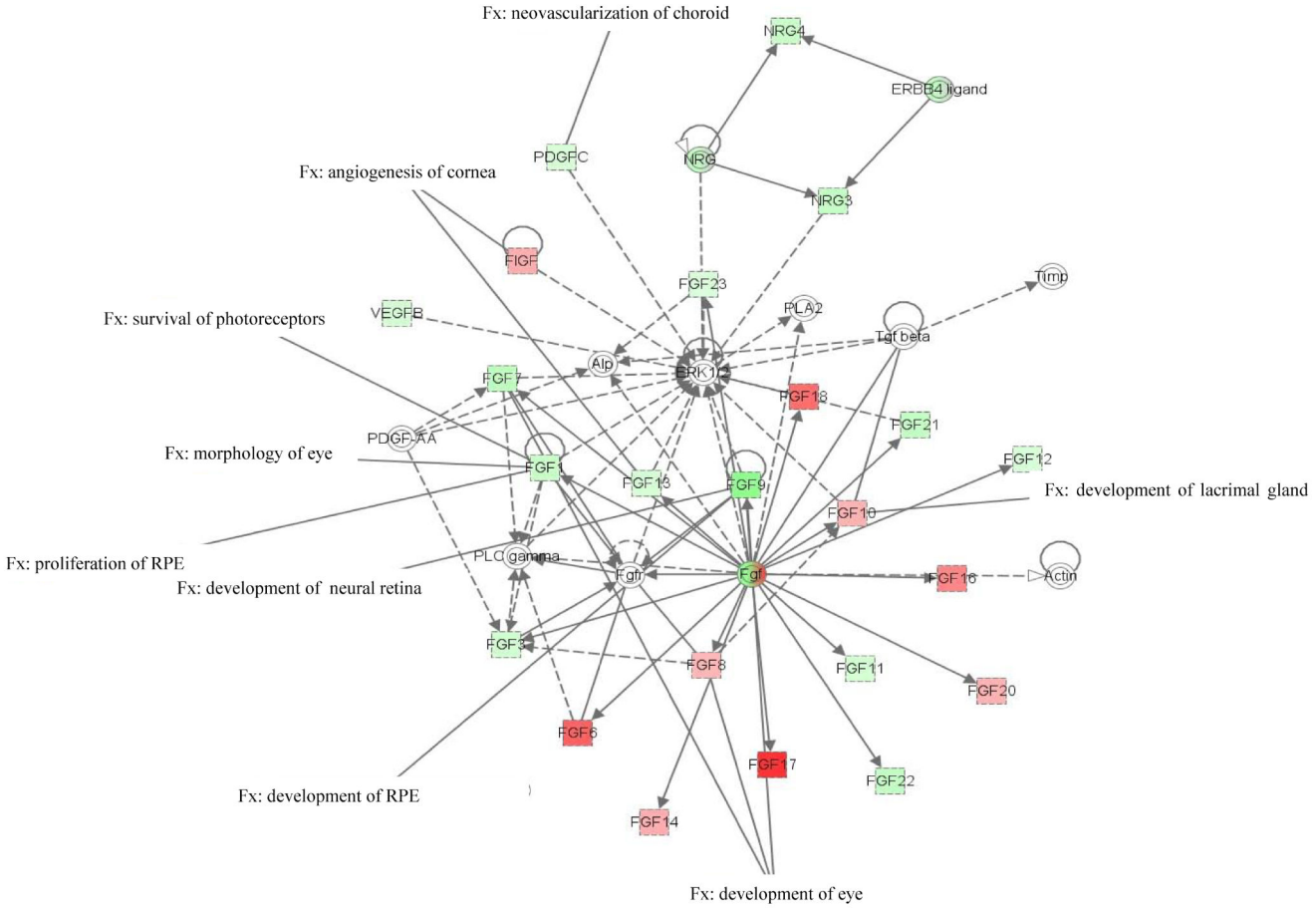

B

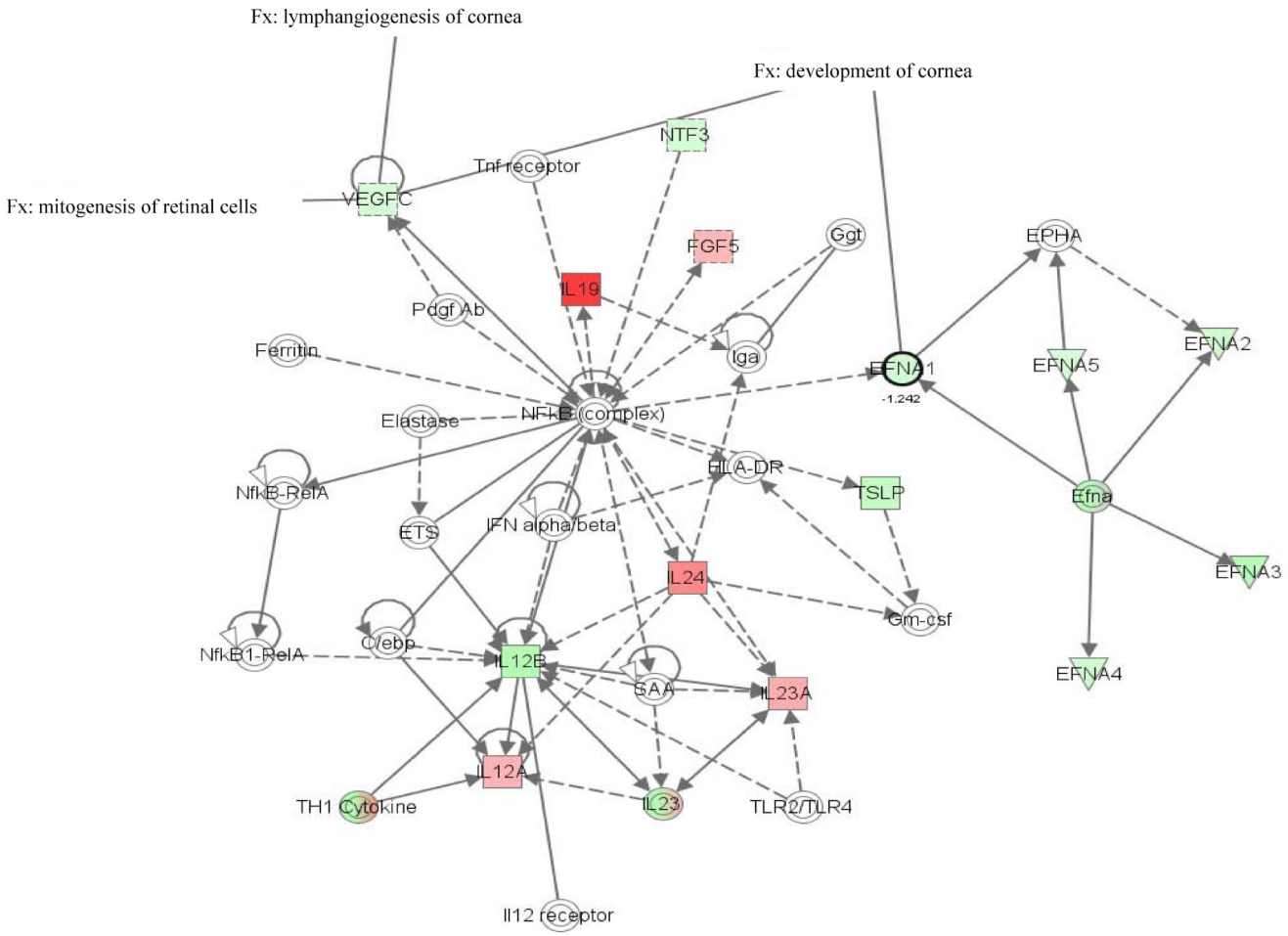

C

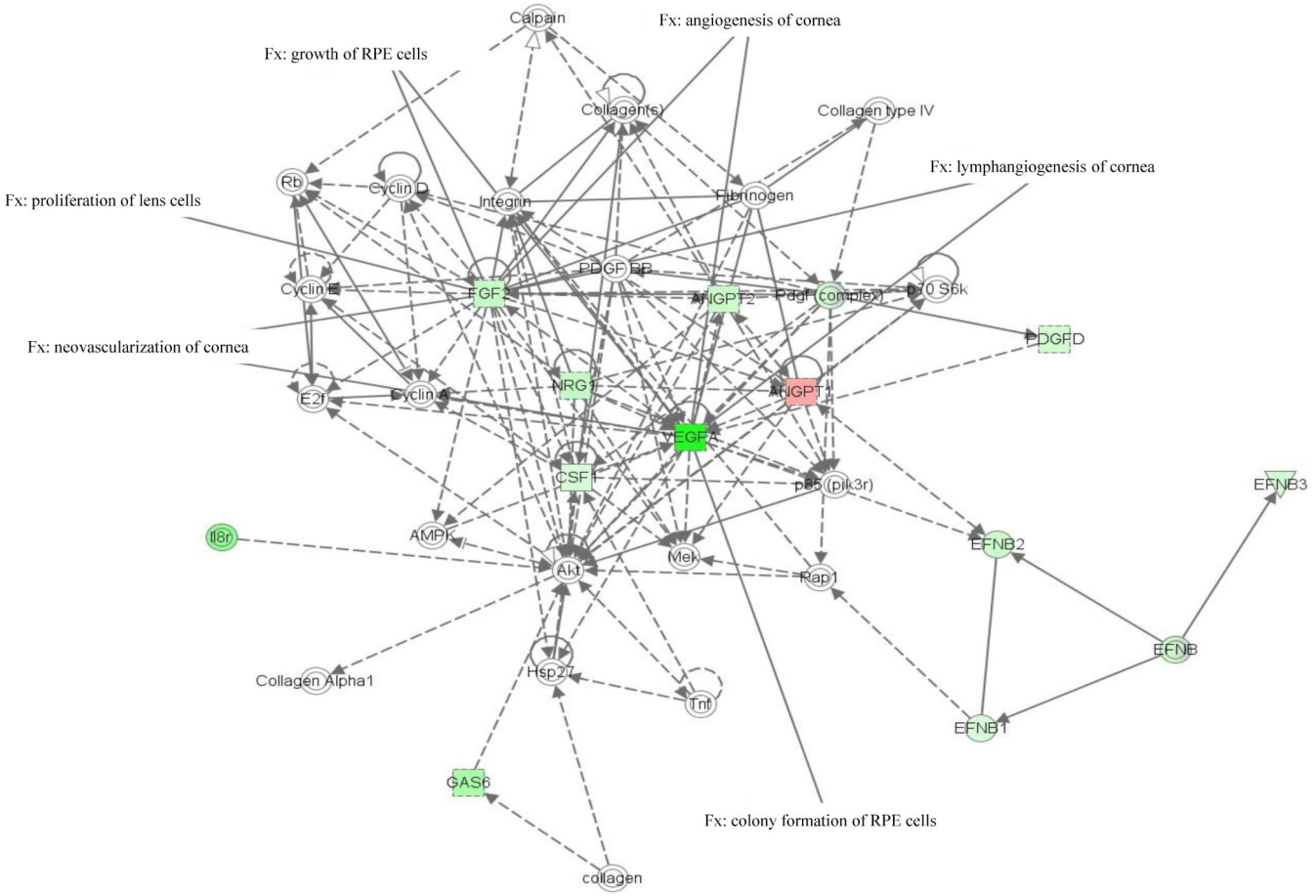

Figure 1. Networks 1(A), 2 (B) and 4 (C) generated by IPA and associated with up- and down-regulated genes in the category visual system and development in the retina of nanoceria injected *Vldlr*−/− mouse

The solid arrow between molecules depicts experimentally proven direct relationship. A dashed line depicts indirect interaction based on experimental evidence. Up-regulated genes are shown in red color and down-regulated in green color. Intensity of color indicates the degree of up- or down-regulation. Genes associated with visual system and development functions are annotated (Fx).

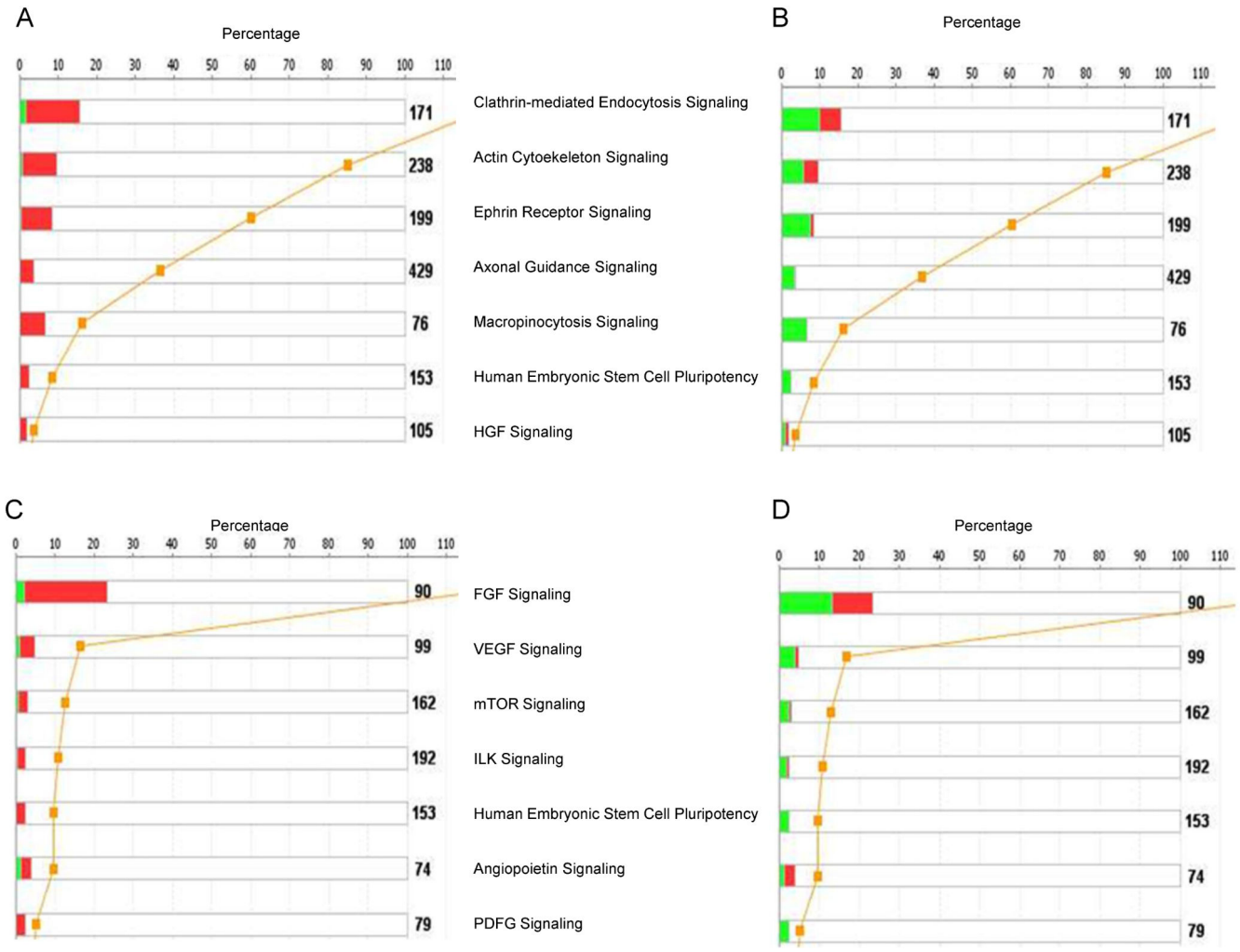

Figure 2. Canonical pathways identified by IPA associated with organismal growth and development (A, B), and cellular growth, proliferation and development (C, D) in the retina of uninjected (A, C) and nanoceria injected (B, D) *Vldlr*−/− mouse

The stack bar chart displays for each canonical pathway the number of genes that are found to be significant. The numerical value at the top of each bar represents the total number of genes/molecules in the canonical pathway. The Benjamini-Hochberg (BH) method was used to adjust the right-tailed Fisher's Exact t-test p-values, which measure how significant each pathway is. Canonical pathway displays the number of up-regulated (red) and down-regulated (green) genes in each canonical pathway. The yellow line represents the threshold p-value.

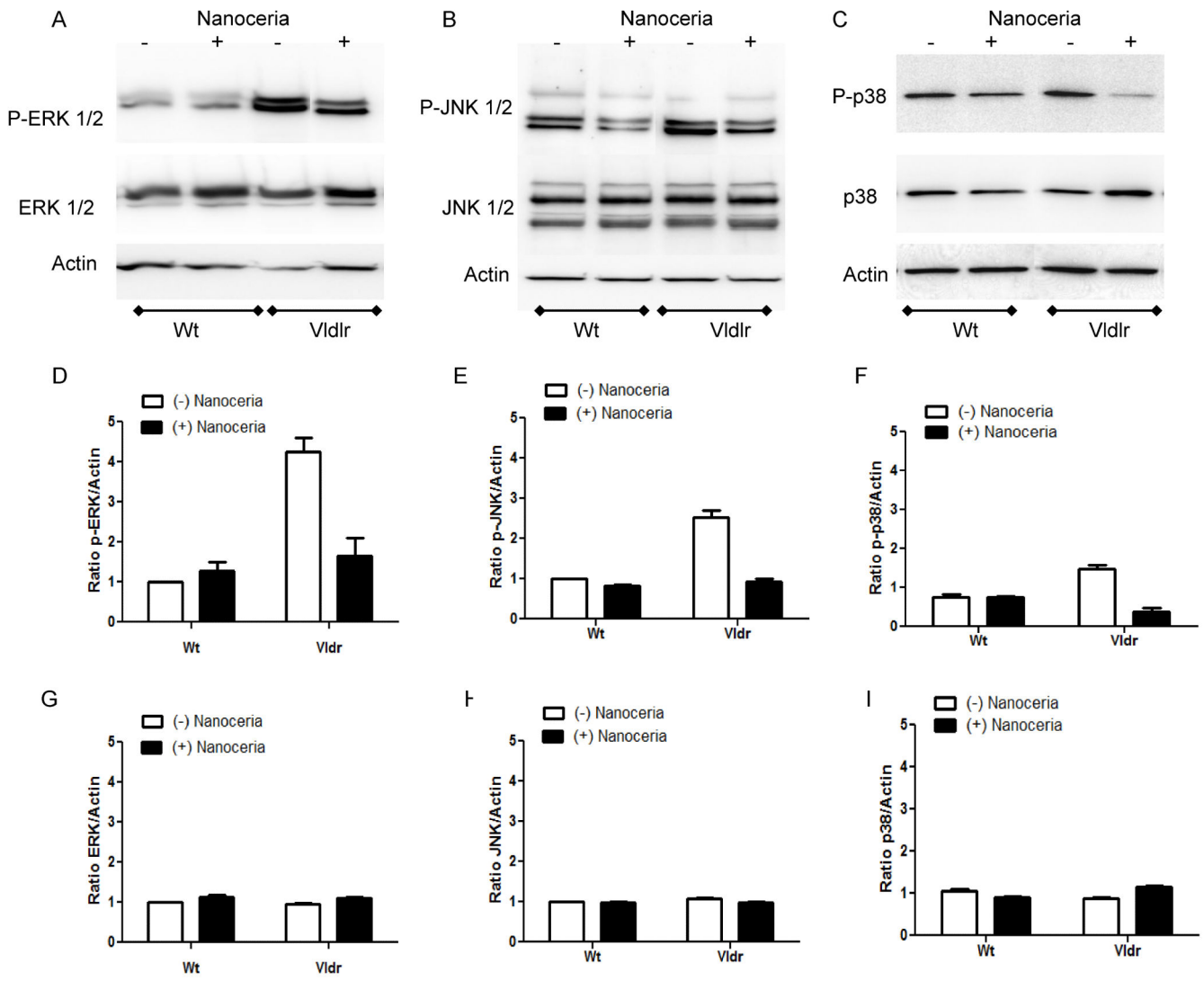

Figure 3. Nanoceria inhibit the activation of MAP kinases in the retina of *Vldlr*−/− mouse

Wt (n=3) and *Vldlr*−/− (n=3) mice were injected with 1μl of 1 mM nanoceria on P28 and the retinas were collected at P35. Uninjected Wt (n=3) and *Vldlr*−/− (n=3) mice at P35 served as controls. Retinal proteins (10μg) were subjected to 10% SDS-PAGE and Western blot analysis for the detection of phosphorylated p-ERK 1/2 (A), p-JNK 1/2 (B) or p-p38 (C) MAP kinases. The same membranes were then stripped and reprobed with anti-ERK 1/2, JNK 1/2 or p38 antibodies, which detect total protein levels, or anti-actin antibody, respectively. The blots were scanned, densitometry analysis performed, and the normalized results are presented as the mean ± S.E.M of the p-ERK/Actin (D), p-JNK/Actin (E), p-p38/Actin (F), ERK/Actin (G), JNK/Actin (H) and p38/Actin (I) ratio from 3 independent experiments.

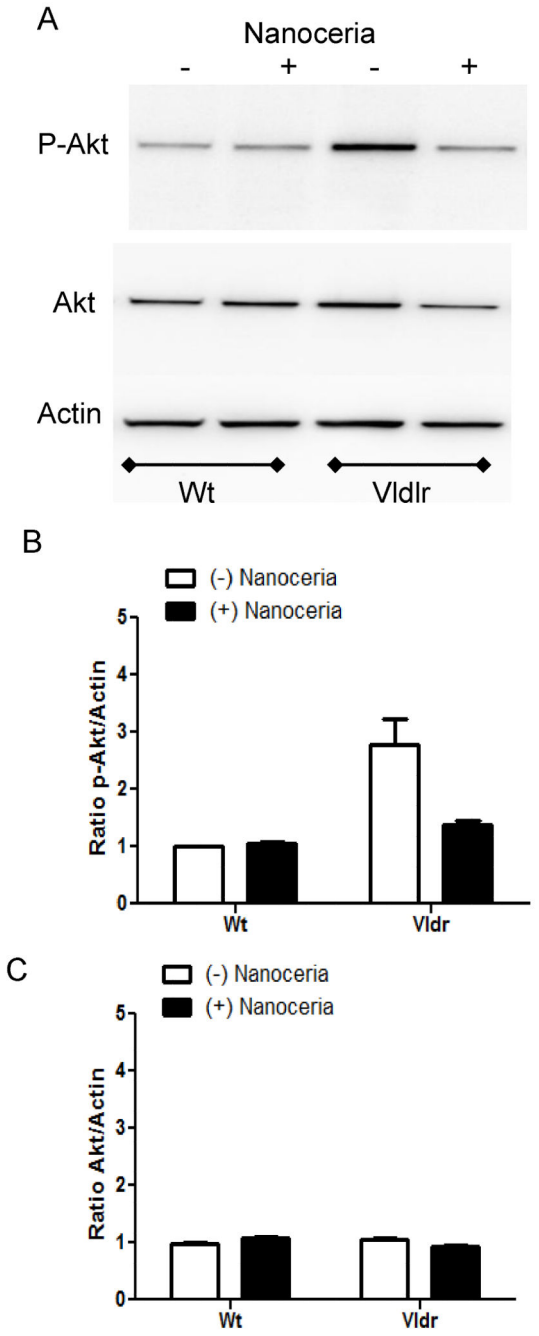

Figure 4. Nanoceria inhibit the activation of Akt in the retina of *Vldlr*−/− mouse

Wt and *Vldlr*−/− mice were injected with 1μl of 1 mM nanoceria on P28 and the retinas were collected at P35. Uninjected Wt and *Vldlr*−/− mice at P35 served as controls. Retinal proteins (10μg) were subjected to 10% SDS-PAGE and Western blot analysis for the detection of phosphorylated p-Akt (A). The same membranes were then stripped and reprobed with anti-Akt antibody which detects total protein levels, or anti-actin antibody, respectively. The blots were scanned, densitometry analysis performed, and the normalized

results are presented as the mean ± S.E.M of the p-Akt/Actin (B) and Akt/Actin (C) ratio from 3 independent experiments.

Table 1

List of differentially expressed genes (≥ 1.5 fold) in the retina of *Vldlr*−/− mice. Data are expressed as fold change of *Vldlr*−/− mice (n=4) to Wt mice (n=4). *P<0.05

Gene name	Gene symbol	*Vldlr*/Wt	
		Fold change	p-value
Up-regulated genes			
Thymic stromal lymphopoietin	*Tslp*	7.8	0.0851
Fibroblast growth factor 7	*Fgf7*	7.0	0.0356*
Fibroblast growth factor 2	*Fgf2*	6.8	0.0233*
Leukemia inhibitory factor	*Lif*	5.9	0.1090
Interferon epsilon 1	*Ifnel*	5.3	0.0464*
Interleukin 3	*Il3*	4.2	0.2062
Fibroblast growth factor 15	*Fgf15*	3.5	0.0415*
Fibroblast growth factor 6	*Fgf6*	2.8	0.1650
Fibroblast growth factor 1	*Fgf1*	2.7	0.0017*
Cardiotrophin-like cytokine factor 1	*Clc*	2.3	0.3340
Fibroblast growth factor 3	*Fgf3*	2.3	0.0602
Growth hormone	*Gh*	2.3	0.5731
Fibroblast growth factor 14	*Fgf14*	2.1	0.0016*
Colony stimulating factor 1	*Csf1*	2.1	0.0560*
Fibroblast growth factor 16	*Fgf16*	2.1	0.4231
Angiopoietin 1	*Angpt1*	2.0	0.1330
Fibroblast growth factor 5	*Fgf5*	2.0	0.0378*
Interleukin 23 a	*Il23a*	2.0	0.1206
Interleukin 6	*Il6*	2.0	0.3177
Ephrin A3	*Efna3*	1.9	0.0283*
C-fos induced growth factor	*Figf*	1.9	0.3595
Fibroblast growth factor 9	*Fgf9*	1.8	0.0402*
Fibroblast growth factor 17	*Fgf17*	1.8	0.0763
Interleukin 19	*Il19*	1.8	0.2910
Interferon gamma	*Ifng*	1.8	0.2202
Neuregulin 3	*Nrg3*	1.8	0.3170
Epidermal growth factor	*Egf*	1.7	0.1051
Interleukin 7	*Il7*	1.7	0.1061
Interleukin 9	*Il9*	1.6	0.0508*
Leptin	*Lep*	1.6	0.1701
Vascular endothelial growth factor A	*Vegfa*	1.6	0.1340
Fibroblast growth factor 20	*Fgf20*	1.6	0.3673
Fibroblast growth factor 21	*Fgf21*	1.6	0.1642
Oncostatin M	*Osm*	1.5	0.1864
Fibroblast growth factor 10	*Fgf10*	1.5	0.1527
Ephrin A1	*Efna1*	1.5	0.0860

Gene name	**Gene symbol**	***Vldlr*/Wt**	
		Fold change	**p-value**
Erythropoietin	*Epo*	1.5	0.0831
Down-regulated genes			
Interleukin 5	*Il5*	−3.4	0.2791
Zing finger protein 91	*Zfp91*	−2.0	0.0380*
Angiopoietin 4	*Angpt4*	−1.8	0.4382
Interleukin 11	*Il11*	−1.8	0.2920
Interleukin 10	*Il10*	−1.8	0.1511

Table 2

List of differentially expressed genes (≥1.5 fold) in the retina of *Vldlr*−/− mice after nanoceria treatment. Data are expressed as fold change of nanoceria (CeO_2) injected *Vldlr*−/− mice (n=6) to Wt mice (n=4). *P<0.05

Gene name	Gene symbol	CeO_2-*Vldlr*/Wt Fold change	p-value
Up-regulated genes			
Fibroblast growth factor 17	*Fgf17*	3.1	0.1742
Interleukin 19	*Il19*	2.9	0.3090
Interleukin 5	*IL5*	2.5	0.2253
Fibroblast growth factor 6	*Fgf6*	2.3	0.0740
Fibroblast growth factor 15	*Fgf15*	2.3	0.3014
Fibroblast growth factor 18	*Fgf18*	2.2	0.1461
Fibroblast growth factor 16	*Fgf16*	1.8	0.0282*
Interleukin 2	*IL2*	1.8	0.1670
Interleukin 24	*IL24*	1.8	0.3723
Interleukin 3	*IL3*	1.7	0.1864
Growth hormone	*Gh*	1.5	0.0890
Interleukin 24	*Il24*	1.5	0.0638
Down-regulated genes			
Vascular endothelial growth factor A	*Vegfa*	−6.2	0.0009*
Interleukin 7	*Il7*	−4.8	0.0410*
Leukemia inhibitory factor	*Lif*	−4.4	0.0192*
Leptin	*Lep*	−3.1	0.1090
Interleukin 9	*Il9*	−3.1	0.0073*
Fibroblast growth factor 9	*Fgf9*	−3.1	0.0871
Epidermal growth factor	*Egf*	−2.4	0.0770
Growth arrest specific 6	*Gas6*	−2.3	0.0104*
Interleukin 12b	*Il12b*	−2.1	0.0750
Ephrin A3	*Efna3*	−2.0	0.1440
Interferon 1	*Ifne1*	−1.9	0.2610
Cardiotrophin-like cytokine factor 1	*Clc*	−1.8	0.2421
Fibroblast growth factor 7	*Fgf7*	−1.8	0.1030
Neuregulin 1	*Nrg1*	−1.7	0.0051*
Neuregulin 3	*Nrg3*	−1.6	0.1652
Thymic stromal lymphopoietin	*Tslp*	−1.6	0.1081
Fibroblast growth factor 21	*Fgf21*	−1.6	0.1000
Fibroblast growth factor 22	*Fgf22*	−1.6	0.2646
Fibroblast growth factor 2	*Fgf2*	−1.6	0.0670
Zinc finger protein 91	*Zfp91*	−1.6	0.0113*
Angiopoietin 2	*Angpt2*	−1.5	0.1080
Fibroblast growth factor1	*Fgf1*	−1.5	0.0261*
Neuregulin 4	*Nrg4*	−1.5	0.0630

Table 3

Top 5 genetic networks in the retina of the *Vldlr*−/− mouse (↑ up- and ↓down-regulation)

Network	Genes	Score	Focus genes	Functions
1	↑Fgf1, ↑Fgf3, ↑Fgf6, ↑Fgf7, ↓Fgf8, ↑Fgf9, ↑Fgf10, ↑Fgf11, ↓Fgf12, ↑Fgf13, ↑Fgf14, ↑Fgf16, ↑Fgf17, ↑Fgf18, ↑Fgf20, ↑Fgf21, ↑Fgf22, ↑Fgf23, ↑Figf, ↑Nrg3, ↑Nrg4, ↑Pdgfc, ↑Vegfb	52	23	Cell-to-cell signaling and interactions, tissue development, cardiovascular system development and function
2	↓Ctf1, ↑Efna1, ↑Efna2, ↑Efna3, ↑Efna4, ↑Efna5, ↑Fgf5, ↓Ifnk, ↑Il19, ↑IL24, ↑IL12a, ↑IL12b, ↑IL23a, ↑Ntf3, ↑Tslp, ↓Vegfc	32	16	Cellular assembly and organization, nervous system development and function, gastrointestinal disease
3	↓Il5, ↑Il7, ↓Il10, ↓Il11, ↓Il13, ↑Il15↑Il20, ↑Lif, ↑Osm, ↓Tpo	18	10	Cell-to-cell signaling and interaction, cellular growth and proliferation, hematological system development and function
4	↓Angpt4, ↓Csf3, ↑Efnb1, ↑Efnb3, ↑Epo, ↑Hgf, ↓Il2, ↑I13, ↑Lep	19	9	Cell-to-cell signaling and interaction, cellular growth and proliferation, hematological system development and function
5	↑Angpt1, ↑Angpt2, ↑Csf1, ↑Efnb2, ↑Fgf2, ↑Gas6, ↑Pdgfd, ↑Vegfa	13	8	Cardiovascular system development and function, cellular growth and proliferation, embryonic development

Table 4

Top 5 genetic networks in the retina of nanoceria injected *Vldlr*−/− mouse (↑up- and ↓down-regulation)

Network	Genes	Score	Focus genes	Functions
1	↓Fgf1, ↓Fgf3, ↑Fgf6, ↓Fgf7, ↓Fgf8, ↓Fgf9, ↑Fgf10, ↓Fgf11, ↓Fgf12, ↓Fgf13, ↑Fgf14, ↑Fgf16, ↑Fgf17, ↑Fgf18, ↑Fgf20, ↓Fgf21, ↓Fgf22, ↓Fgf23, ↑Figf, ↓Nrg3, ↓Nrg4, ↓Pdgfc, ↓Vegfb	52	23	Cell-to-cell signaling and interactions, tissue development, cardiovascular system development and function
2	↓Efna1, ↓Efna2, ↓Efna3, ↓Efna4, ↓Efna5, ↑Fgf5, ↑Il19, ↑IL24, ↑IL12a, ↓IL12b, ↑IL23a, ↓Ntf3, ↓Tslp, ↓Vegfc	28	14	Cellular assembly and organization, nervous system development and function, gastrointestinal disease
3	↓Ctf1, ↑Epo, ↑Il5, ↓Il7, ↓Il10, ↓Il11, ↑Il13, ↑Il15, ↓Il20, ↓Lif, ↓Osm, ↓Tpo	23	12	Cell death, growth and proliferation, hematological system development and function
4	↓Angpt1, ↓Angpt2, ↓Csf1, ↓Efnb1, ↓Efnb2, ↓Efnb3, ↓Fgf2, ↓Gas6, ↓Nrg1, ↓Pdgfd, ↓Vegfa	20	11	Cardiovascular system development and function, embryonic development, tissue development
5	↓Cls, ↓Fgf13, ↑Ifng, ↓Il9, ↑Il19, ↓Ill20, ↓Zfp91	11	7	Cellular development, growth and proliferation, connective tissue development and function